

## Investigation of the dynamics of drug delivery systems by electron and optical microscopy

© N.N. Sudareva,<sup>1</sup> O.M. Suvorova,<sup>1</sup> N.N. Saprykina,<sup>1</sup> K.A. Kolbe,<sup>1</sup> N.V. Smirnova,<sup>1</sup> D.N. Suslov<sup>2</sup>

National Research Center „Kurchatov Institute“,  
199004 SPb, Russia

<sup>2</sup> National Medical Resesarch Center of Oncology named after N.N.Petrov,  
197758 SPb, Russia  
e-mail: nnsas@mail.ru

Received February 28, 2024

Revised June 8, 2024

Accepted July 8, 2024

Microscopy methods of different resolutions were used to record the dynamics of the following processes occurring with drug delivery systems (DS) *in vitro* and *ex vivo*: 1) a time change in the structure of DS of the antitumor antibiotic doxorubicin based on particles of porous calcium carbonate vaterites doped with polyanion dextran sulfate and hydroxyapatites under the influence of blood plasma (evaluated using a scanning electron microscope); 2) an increase in five times the size of alginate granules — potential carriers of wound healing drugs — in the medium of exudate (wound fluid) (observed in an optical microscope); 3) spatial distribution of fluorescently labeled protein in the volume of particles of porous CaCO<sub>3</sub> vaterite (presented in the form of optical slices obtained using a laser scanning confocal microscope); 4) the effect of doxorubicin concentration increasing to 2 μg/ml, encapsulated in porous vaterite particles, on dermatocarcinoma A431 cells, cell death after four days in a nutrient medium with DS (studied using a light inverted microscope); 4) interaction of DS with macrophage cells obtained from the human leukemia monocyte cell line THP-1 MF and their uptake of DS after 24 h of joint incubation (demonstrated using an optical microscope with fluorescence detection).

**Keywords:** delivery systems, doxorubicin, scanning electron microscopy, light inverted microscopy, fluorescent and laser scanning confocal microscopy.

DOI: 10.61011/TP.2024.09.59287.55-24

### Introduction

Microscopy methods with different resolutions are used to determine the parameters of drug compound delivery systems (DS). Scanning electron microscopy (SEM), transmission electron microscopy (TEM) and atomic force microscopy (AFM) can characterize the size, morphology, porosity, and surface structure of objects [1]. Laser scanning confocal microscopy (LSCM) is used to detect the presence and position of DS components labeled with fluorochromes [2,3]. Obtaining information about the structures of various delivery systems is a necessary step to understand their functioning in the body. The use of electron and optical microscopy methods helps to evaluate the effectiveness of delivery systems.

The main object whose behavior *in vitro* and *ex vivo* has been studied using microscopy of different resolutions are drug delivery systems based on calcium carbonate (CaCO<sub>3</sub>). They are widely used in healthcare [4,5]. Delivery systems protect drug compounds from the effects of the body's environment, prolong their release and, thus, allow large concentrations of drugs to be administered without fear of overdose. There are three morphological modifications CaCO<sub>3</sub> that are clearly distinguishable using SEM — spherical porous vaterites, nonporous calcites and aragonites

that transform into each other under different conditions. There are several options for including drug compounds in vaterites: co-precipitation, diffusion, centrifugation. The morphological uniformity of delivery systems affects the amount of loading of biologically active substances. For example, the loading of proteins in DS by the method of co-deposition at a maximum of 100% vaterite content, an increase in the part of calcites in the carriers reduces the loading of [6]. The LSCM method demonstrates the presence of fluorochrome-labeled proteins in DS from CaCO<sub>3</sub>vaterites coated with a multilayer polyelectrolyte shell, also with labeled polymers [3].

In the process of diffusion loading of the anticancer drug doxorubicin (DOX) in the form of hydroxide, a partial transformation of the carrier structure occurs. It was shown using SEM that when DOX is loaded into vaterites CaCO<sub>3</sub>, the latter dissolve with subsequent recrystallization into the form of non-porous calcites due to the increased acidity of the medium, while the amount of DOX included decreases. The CaCO<sub>3</sub> vaterites were coated with dextran sulfate (CaCO<sub>3</sub>+DXS) polyanion for protection of the DS structure [7]. The loading of vaterite in calcium alginate granules was another option for protecting vaterites particles from environmental impact, for example, gastric acidity in case of oral administration of DS therapeutic peptides [8].

Alginate, like dextran sulfate, is a biodegradable non-toxic polymer used not only as components of DS, but also in wound healing processes. The wound healing process contains three main stages, and in each of them it is possible to introduce an appropriate drug. It is necessary to introduce an antiseptic in the first stage— inflammatory stage. The second and third stages — regeneration and epithelialization — require the addition of biologically active substances (BAS) that stimulate the corresponding processes. Therapeutic peptides of various structures play an important role here [9,10]. They are injected into the wound directly or in microparticles of polylactide-co-glycolide or hyaluronic acid [11,12]. The wound healing is accelerated in case of usage of growth factor-saturated emulsion microspheres made of polylactide-co-glycolide with addition of alginate [13]. Calcium alginate granules [14], produced under the name Migran [15], have broad opportunities for use in healthcare. In recent years, the use of BAS carriers in medicinal dressings made of hydrogel and alginate materials has been expanding, which provide a suitable moist environment, have good biocompatibility and high swelling rate for the absorption of exudate [16–18]. As we can see, the loading of therapeutic peptides in alginate carriers increases the effectiveness of their action in wounds. Therefore, it is important to study the effect of exudate — contents of wounds — on alginate carriers during their interaction over time.

Experiments *ex vivo* help to evaluate the effectiveness of DS in their interaction with cells.

The effect of toxic compounds on cells is usually assessed using such parameter as the „viability“, reflecting the proportion of viable cells after exposure to a certain concentration of the drug. The methyl tetrazolium test (MTT) or the xCELLigence system is used to quantify the process. MTT is a colorimetric test based on the reduction of yellow tetrazole into purple insoluble formazane by living cells. The optical density of the formazane solution in dimethyl sulfoxide, determined at 570 nm, characterizes the number of living cells [19]. The use of the xCELLigence system, the principle of operation of which is based on changing the impedance of gold sensors when dead cells are disconnected from them, allows determining cytotoxicity in real time [20]. An example of the use of optical microscopy to assess the effect of the studied drugs on the morphological state of the cells of an organ undergoing treatment is given in Ref. [21].

The direct interaction of DS with cells, or their uptake, can be seen through the use of laser confocal scanning microscopes (LCSM) [1,22]. These devices were created to study the structure of an object in three-dimensional space. Obtaining an image of a cell from different angles [23] allows understanding whether the DS is included in the cell or is located on its surface. One of the few disadvantages of LCSM is the need to use fluorescent labels. The various objects under study should be labeled with fluorochromes detected in different wavelength ranges. A specific problem should also be mentioned — compounds

(in particular proteins) with attached fluorescent labels can change their structure, which may affect their interaction with surrounding objects [24].

The task of this work is to understand the change of the structure of drug delivery systems during their existence. Namely, from their creation and loading of drug compounds through obstacles created by the body's environments, to inclusion of DS in cells and the realization of the activity of encapsulated drug compounds. The use of microscopes with different detection methods and a wide range of resolution makes it possible to control the size and structure of delivery systems at different stages of their existence.

## 1. Results and discussion

### 1.1. Changes of the structures of doxorubicin delivery systems in blood plasma over time

Control using SEM of DS based on particles of  $\text{CaCO}_3$  which were used as carriers of nucleic acids, therapeutic proteins, peptides, and the antitumor drug doxorubicin (DOX), showed their effectiveness both *in vitro* and *in vivo* [1,2,8,25]. DOX was also loaded in porous carriers of a different composition — hydroxyapatites (HA) formed during treatment of  $\text{CaCO}_3$  with phosphorus salts. The sizes of these carriers are close, the porosity is slightly higher for HA, and the loading of DOX in HA particles is 30% lower than in particles of  $\text{CaCO}_3$  [26]. However, the profiles of DOX release into the blood *in vivo* differ significantly. The method of high-performance liquid chromatography did not detect DOX in blood plasma for 25 days after its intraperitoneal administration using HA. At the same time, the use of  $\text{CaCO}_3$ +DXS ensures a prolonged (up to 20 days) release of DOX into the blood of rats. The amount of DOX administered is the same in both cases is 4 mg per rat. Let us recall that free DOX is released into the blood of a rat three days after intraperitoneal administration. The cause of the differences was determined using SEM images of both structures, which change differently with time in the blood. Figure 1 demonstrates the structures of  $\text{CaCO}_3$ +DXS and HA — intact (A and C) and after their interaction with blood plasma for a week *in vitro* (B and D). Fig. 1 shows differences in the intensity of destruction of both DS, which can explain the differences in the results of *in vivo* experiments. Vaterite particles are destroyed into small fragments, the polyelectrolyte shell of DXS no longer completely covers the cores of  $\text{CaCO}_3$ . This allows the release of DOX into the blood plasma. The size of HA particles practically does not increase during the seven days in the blood plasma. The porosity of the structure increases. DOX is not released from HA particles, which can be explained by sorption.

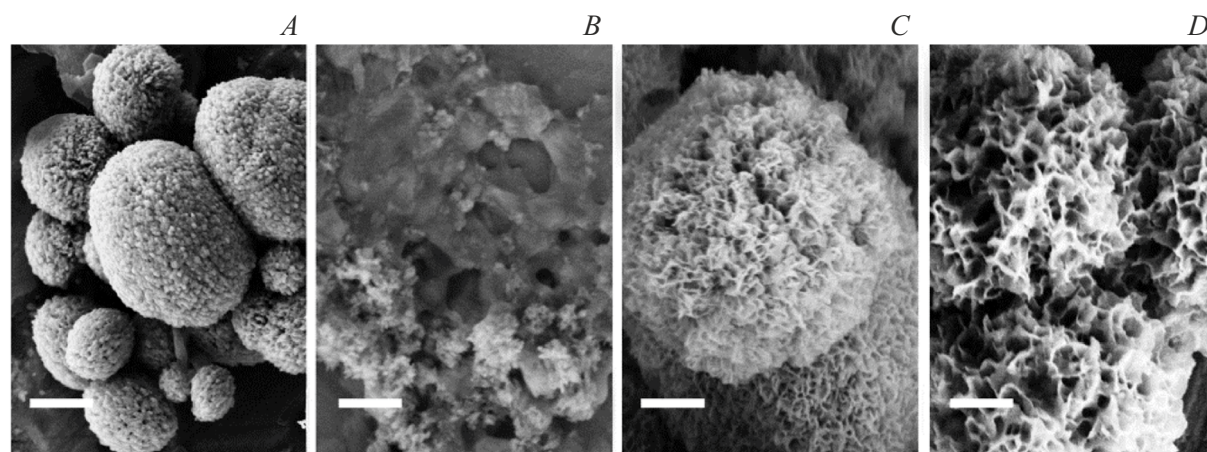


**Figure 1.** Original DS: *A* —  $\text{CaCO}_3$ +DXS; *C* — HA. After 7 days in blood plasma: *B* —  $\text{CaCO}_3$ +DXS; *D* — HA. Marker — 1  $\mu\text{m}$ .

### 1.2. Loading of proteins in $\text{CaCO}_3$ vaterites. Control with LSCM

The spatial dynamics of the protein location in the carrier volume is demonstrated in Fig. 2. Loading of bovine serum albumin (BSA) labeled with fluorescein isothiocyanate (FITC) in the ratio (BSA:FITC= 1:15), in  $\text{CaCO}_3$  vaterite particles, the co-precipitation method was controlled using the optical cross-section technique on LSCM. The slice step is 0.20  $\mu\text{m}$  which is greater than the resolution of the microscope 0.16  $\mu\text{m}$  (see Appendix), which allows obtaining the most informative slices [27].

It can be seen in the series of photos (Fig. 2) that the protein fills the entire volume of vaterite particles, sometimes unevenly. The distribution of drug compounds encapsulated in  $\text{CaCO}_3$  looks differently in publications where their LSCM photos are provided. In one case [2] siRNAs (small interfering ribonucleic acids) with a fluorescent marker (PA-1630-FAM) are distributed very unevenly in  $\text{CaCO}_3$  vaterite particles. LSCM photo of particles of  $\text{CaCO}_3$  with encapsulated human serum albumin labeled with FITC demonstrates uniform distribution of protein [3]. In both cases, the loading of labeled objects was performed using the co-deposition method. The magnifications in the cited papers are close, which makes it possible to compare the images shown in them.

### 1.3. Uptake of $\text{CaCO}_3$ +DXS delivery systems by cells

The antitumor antibiotic doxorubicin exhibits cytotoxicity precisely at the stage of cell division. DOX when included between the chains of deoxyribonucleic acid (DNA), disrupts the processes of replication and transcription and, thus, inhibits tumor growth. Capture of DOX delivery systems based on  $\text{CaCO}_3$ +DXS vaterite by THP-1 MF cells was demonstrated using a direct fluorescence microscope. The photos were processed using ZEN software (blue edition).

A comparison of the photos in Fig. 3 indicates the loading of DS based on  $\text{CaCO}_3$ +DXS in cells during a day.

Various fluorescent dyes were used to detect cells and their interaction with delivery systems. Prior to the addition of DS, the cells were treated with the fluorescent dye Texas Red-X, which contrastingly stains the cytoskeleton of the cell. The delivery systems were stained with PKH26 dye. They were used without the addition of DOX, so that its own fluorescence would not complicate the interpretation of the results. The uptake did not yet occur during 20 min after the addition of DS to the cells, and DS is distributed throughout the volume (Fig. 3*B*), whereas DS penetrated into the cells after 24 h (Fig. 3*C*). The cells were thoroughly washed during the day after contact with DS. It can be assumed based on the absence of DS around the cells that all loose DS were removed, only those that got inside the cells remained in place. Thus, it can be assumed that the combined images of cells and DS in Fig. 3*C* reflect the loading of DS in cells.

In the future, it will be necessary to compare uptake of DS based on  $\text{CaCO}_3$ +DXS not only by macrophages, but also by other cells — cancerous — MCF7 or A431 and fibroblasts. The selection of the necessary fluorophores will help determine the capture of DS with DOX by cells.

### 1.4. The effect of the encapsulated antitumor antibiotic doxorubicin on cells

The interaction of cells with DS containing DOX leads to disruption of their functioning. In a cellular environment, a light microscope allows estimating the concentration dynamics of the toxicity of DOX encapsulated in  $\text{CaCO}_3$ +DXS delivery systems in relation to epidermoid carcinoma cells A431 (Fig. 4). The morphology of cells changes under the impact of an ever-increasing concentration of DOX.

Fig. 4 shows optical photographs of cancer cells (epidermoid carcinoma) A431 on the third day of their contact with DOX administered with  $\text{CaCO}_3$ +DXS, with an increase of the concentration of the drug to 2.0  $\mu\text{g}/\text{ml}$ . Fig. 4*A* shows

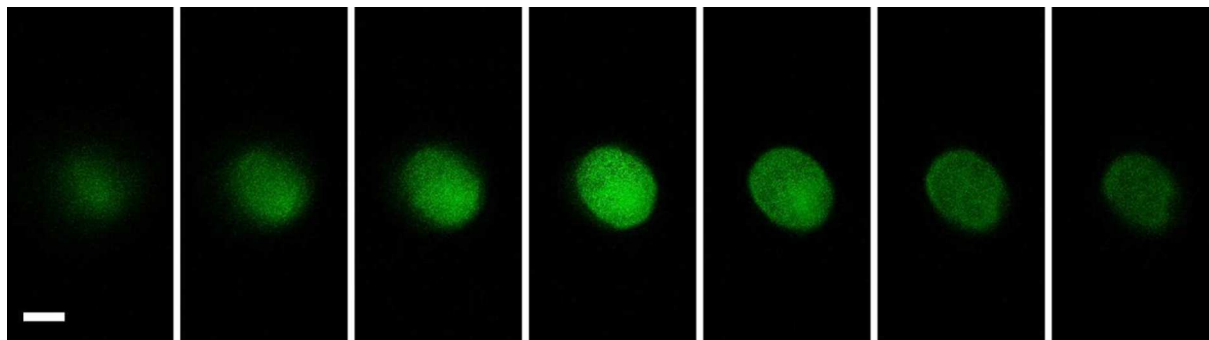


**Figure 2.** LSCM photo of optical slices of  $\text{CaCO}_3$  vaterites with encapsulated BSA labeled by FITC. Marker —  $2 \mu\text{m}$ .

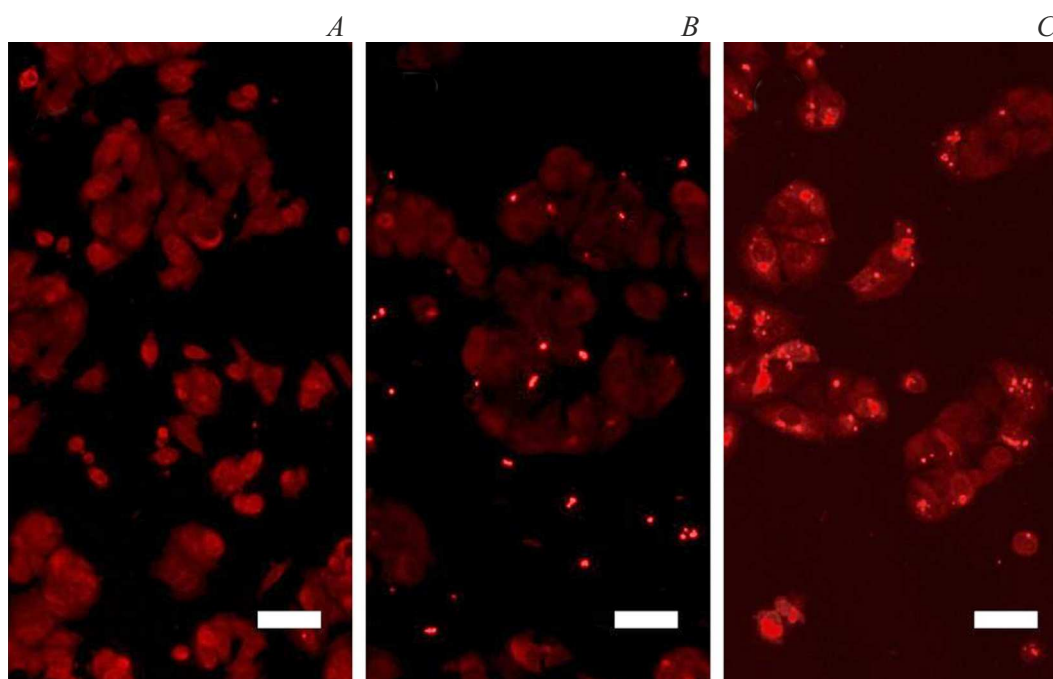


**Figure 3.** Photos of THP-1 MF cells before the addition of DS (A) and after the addition of DS and their joint incubation for 20 min (B) and 24 h (C). Marker —  $50 \mu\text{m}$ .

original healthy cells are visible spread out on the surface of the substrate, which form a cellular monolayer. The distance between viable cells increases with an increase of the concentration of DOX to  $0.50 \mu\text{g/ml}$  (Fig. 4, C) due to a decrease of the number of viable cells, the cells change morphology (area „alive“ in fig. 4, C). Some of the dead cells detached themselves from the surface and aggregated (area „dead“ on fig. 4, C). All the cells died at the maximum concentration of DOX used ( $2.0 \mu\text{g/ml}$ ), they detached themselves from the surface, and stuck together (Fig. 4, D).

### 1.5. Change of the structure of an alginate granule — a potential drug carrier in exudate in time

The addition of alginate increases the effectiveness of the wound treatment process in case of usage of drug

compound carriers or wound healing dressings. If drug compounds, such as peptides, are included in calcium alginate granules, then their release depends on a change in the structure of the carrier in the surrounding wound environment. Exudate is a fluid accumulating in wounds during the inflammatory process. Its composition may vary depending on the stage of the inflammation process. The exudate formed after the burn was used in this paper, the pH value of which is about 7. The effect of exudate on alginate was assessed by the swelling of alginate granules for two days based on their photographs obtained using a light inverted microscope (Fig. 5). The granules contained no medicinal compounds. The release of drugs from calcium alginate granules was demonstrated in Ref. [28].

It can be seen from the graph in Fig.5 that a fivefold increase in the size of granules takes place in two days. In addition to the release of encapsulated drugs, when the



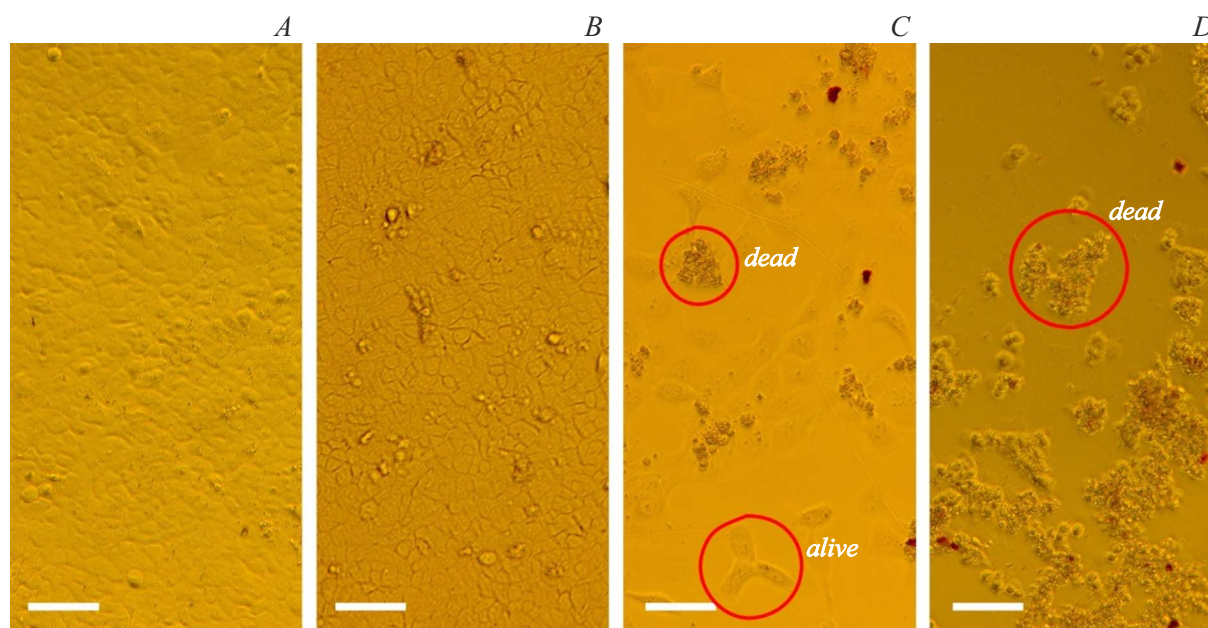


**Figure 4.** A change in the morphology of epidermoid carcinoma cells A431 after their contact with DS containing DOX. DOX concentration of 0.05 (B), 0.50 (C) to 2.0 (D)  $\mu\text{g/ml}$ . A — cells without DS. Marker — 100  $\mu\text{m}$ .

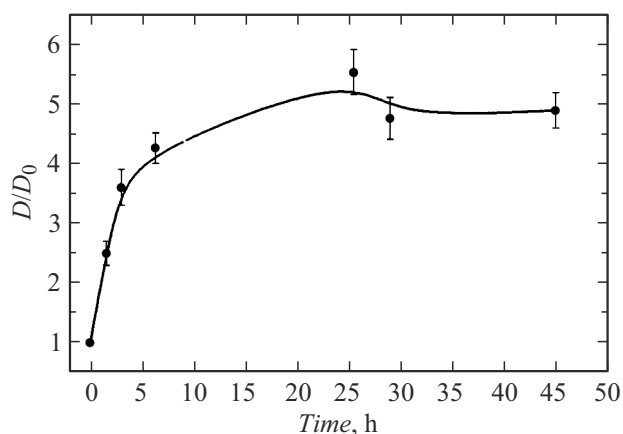


**Figure 5.** Dynamics of alginate granule size increase in exudate.

granules swell, effective absorption of exudate takes place, i.e., drying of the wet wound.

## Conclusion

Microscopy of various resolutions accompanies drug delivery systems *in vitro* from the moment of their formation and the loading of drugs in them to their destruction under the influence of various body media, such as blood plasma or the environment of the gastrointestinal tract. Microscopy also allows *ex vivo* controlling the effects of DS on cells of various natures (both healthy and cancerous) and to take into account the duration of interaction of cells with DS and the amount of drugs released from DS. The totality of such

information helps to assess the effectiveness of the delivery systems being developed.

## Appendix. Materials and methods

Salts used for the synthesis of porous carbonate cores  $\text{CaCl}_2 \cdot 2\text{H}_2\text{O}$  and  $\text{Na}_2\text{CO}_3$ , polyanion dextran sulfate were produced by Sigma-Aldrich (USA). Syndroxocin produced by Actavis (Hafnarfjordur, Iceland) contained 17% DOX in the form of a salt with a protonated amino group and 83% lactose. The sodium salt of alginate (for medical use, MM about 300 kDa) is produced by the Arkhangelsk Algae Experimental Plant (Russia). The exudate, in which the swelling of alginate granules was determined for two days, was obtained from the I.I. Janelidze Institute of Emergency Medicine.

Alginate granules as fillers of burn wounds were produced by ion crosslinking, namely, a 4% aqueous solution of alginate was added by digging into a sedimentation bath with 5% calcium chloride, after 30 min of stirring, the suspension was filtered on a Buchner funnel, washed with water and dried in air.

The synthesis of  $\text{CaCO}_3$  porous vaterites was carried out according to a modified technique [29], namely, the co-precipitation of 1 M solutions of  $\text{CaCl}_2 \cdot 2\text{H}_2\text{O}$  and  $\text{Na}_2\text{CO}_3$  was carried out by stirring by a mechanical stirrer at 2000 rpm for 30 s, the precipitate was washed three times using centrifugation and drying. Dextran sulfate was applied to the surface of the vaterite during mixing of the suspension of  $\text{CaCO}_3$  in an aqueous polymer solution with a concentration of 2 mg/ml for 1 h. This was followed by thorough washing and drying.

The hydroxyapatites used in this paper were manufactured as follows.

A suspension of 0.5 M CaCO<sub>3</sub> (in the form of vaterite particles manufactured according to the above procedure) was added to 0.1 M solution of Na<sub>2</sub>HPO<sub>4</sub> in a molar ratio of 1:1. The subsample was treated by ultrasound for 20 s, then stirred for 24 h, centrifuged for 5 min at  $8 \cdot 10^3$  rpm, the precipitate was washed with water three times and dried to constant weight.

The loading of DOX in the DS was performed by diffusion with stirring during the day of a suspension of CaCO<sub>3</sub>+DXS and a solution of DOX. The ratio of components varied depending on the required amount of DOX in DS. The amount of loaded DOX was determined spectrophotometrically by the difference between the original and non-included DOX DS based on calibration at  $\lambda = 480$  nm.

### P1. Working with cells

Epidermoid carcinoma A431 cells and macrophage cells derived from the human leukemia monocytic cell line THP-1 MF were provided by the Institute of Cytology of the Russian Academy of Sciences from the Russian Collection of vertebrate Cell cultures.

The dynamics of A431 cell proliferation was evaluated when they were conditioned with CaCO<sub>3</sub>+DXS carriers containing different amounts of DOX. The cells were cultured in a complete DMEM culture medium (Paneco, Russia) with the addition of 1% L-glutamine 200 mm, 10% bovine embryonic serum and 1% antibiotics (100 units/ml penicillin, 100  $\mu$ g/ml streptomycin), 1% antimycotic (amphotericin B 250  $\mu$ g/ml) (all reagents produced by Thermo Fisher Scientific, USA). Cultivation was carried out in a CO<sub>2</sub> incubator (Thermo Fisher Scientific, USA) at a temperature of 37°C, concentration of CO<sub>2</sub> 5% and high humidity. 35 thousand A431 cells were placed in each cell with a cultural medium (volume 0.2 ml). A day later, empty DS and DS containing varying amounts of DOX were added to the cells, obtained during three days of contact of A431 cells with different variants of DS. The interaction of DS containing different amounts of DOX with A431 cells is reflected by lifetime micrographs obtained using Primo Vert inverted light microscope (Carl Zeiss, Germany). 100 x magnification.

An increase of the size of alginate granules under the influence of an exudate medium was determined according to the photographs obtained using the same microscope at different time intervals.

Fluorescent detection. Prior to the addition of DS, THP-1MF cells were stained with the fluorescent dye Texas Red-X ( $\lambda$  excitation= 561 nm, emission= 615 nm). DS was labeled with the red fluorescent dye PKH 26 ( $\lambda$  excitations= 550 nm, emissions= 567 nm) using reagents and techniques from the labeling kit (Sigma-Aldrich, USA). The delivery systems were captured by cells under the following conditions. After culturing of 35 thousand per cell in

a complete cultural medium during the day, CaCO<sub>3</sub>+DXS was added to them at a concentration of 10  $\mu$ g/ml. After a day of interaction of the cells with DS, they were thoroughly washed from the culture medium containing DS and images were taken using ZEISS Axio Scope A1 light microscope (Carl Zeiss, Germany) with fluorescent detection.

### P2. Microscopy

Scanning electron microscope SEM Supra 55VP (Carl Zeiss, Germany) in the secondary electron mode was used to determine changes of the microstructures of delivery systems of different compositions, namely porous calcium carbonate vaterites and hydroxyapatites in contact with human blood plasma. A thin layer of platinum was applied to the surface of the sample before measuring.

A series of optical slices CaCO<sub>3</sub> containing BSA labeled by FITC ( $\lambda$  excitations= 495 nm, emissions= 519 nm) was obtained on the LCSM LSM 5 PASCAL (Leica Microsystems, Germany) in Z-stack mode using an argon laser. The thickness of the optical slice is 0.2  $\mu$ m. The resolution ( $d$ ), according to the Helmholtz formula, is equal to  $(0.61 \cdot \lambda)/(n \cdot \sin \alpha)$ . With the laser used ( $\lambda = 405$  nm) and the microscope design (aperture angle  $\alpha = \pi/2$ ; oil immersion  $n = 1.5$ ), the resolution was 0.16  $\mu$ m, which is less than the thickness of the optical slice and is about 5% of the average particle size of vaterite CaCO<sub>3</sub>, equal to 2–4  $\mu$ m.

### P3. Working with laboratory animals

Healthy rats from the Rappolovo laboratory animal nursery were used in experiments on intraperitoneal injection of various doxorubicin delivery systems into the blood of animals. All manipulations with rats were performed under general anesthesia. The work with animals was carried out in accordance with the rules for the use of experimental animals (according to the principles of the Helsinki Declaration of the World Medical Association on the Humane Treatment of Animals, 1996,).

### Funding

The work was carried out within the scope of the state assignment of the scientific research center „Kurchatov Institute“ on the topic „Polymers for biomedicine“, registration number 124013000730-3.

### Conflict of interest

The authors state that they have no conflict of interest.

### References

- [1] Y.V. Taranchikova, D.S. Linnik, T. Mashel, A.R. Muslimov, S. Pavlov, K.V. Lepik, M.V. Zyuzin, G.B. Sukhorukov, A.S. Timin. Mater. Sci. Eng. C, **126**, 112161 (2021). DOI: 10.1016/j.msec.2021.112161

- [2] A.S. Timin, A.R. Muslimov, A.V. Petrova, K.V. Lepik, M.V. Okilova, A.V. Vasin, B.V. Afanasyev, G.B. Sukhorukov. *Sci. Rep.*, **7**, 102 (2017). DOI: 10.1038/s41598-017-00200-0
- [3] M.V. Zyuzin, D. Antuganov, Y.V. Tarakanchikova, T.E. Karpov, T.V. Mashel, E.N. Gerasimova, O.O. Peltek, N. Alexandre, S. Bruyere, Y.A. Kondratenko, A.R. Muslimov, A.S. Timin. *ACS Appl. Mater. Interfaces*, **12**, 31137 (2020). DOI: 10.1021/acsami.0c06996
- [4] D.B. Trushina, T.V. Bukreeva, M.V. Kovalchuk, M.N. Antipina. *Mater. Sci. Eng. C*, **45**, 644 (2014). DOI: 10.1016/j.msec.2014.04.050
- [5] A.D. Trofimov, A.A. Ivanova, M.V. Zyuzin, A.S. Timin. *Pharmaceutics*, **10**, 167 (2018). DOI: 10.3390/pharmaceutics10040167
- [6] N.N. Sudareva, E.V. Popova, N.N. Saprykina. *Fiziko-himiya polimerov. Sintez, svojstva i primenenie*, **20**, 139 (2014) (in Russian).
- [7] N. Sudareva, O. Suvorova, N. Saprykina, H. Vlasova, A. Vilesov. *J. Microencaps.*, **38** (3), 164 (2021). DOI: 10.1080/02652048.2021.1872724
- [8] N. Sudareva, O. Suvorova, N. Saprykina, N. Smirnova, P. Bel'tiukov, S. Petunov, A. Radilov, A. Vilesov. *J. Microencaps.*, **35** (7–8), 619 (2019). DOI: 10.1080/02652048.2018.1559247
- [9] L. Chan, S. Gunasekera, S. Henriques, N. Worth, S. Le, R. Clark. *Blood*, **118**, 6709 (2011). DOI: 10.1182/blood-2011-06-359141
- [10] K. Ito, Y. Matsuda, A. Mine, N. Shikida, K. Takahashi, K. Miyairi. *Commun. Biol.*, **5**, 56 (2022). DOI: 10.1038/s42003-022-03015-6
- [11] K. Stashevskaya, E. Markvicheva, S. Strukova, A. Rusanova, A. Makarova, L. Gorbacheva, I. Prudchenko, V. Zubov, K. Grandfis. *Biochem. Moscow Suppl. Ser. B*, **1**, 147 (2007). DOI: 10.1134/S1990750807020072
- [12] S. Kang, J. Choi, H. Kim, J. Seo, S. Park, E. Kim, S. Park, K. Huh, H.-M. Chung, H.-Y. Chung, S. Moon. *Part. Part. Syst. Charact.*, **34**, 1600320 (2017). DOI: 10.1002/ppsc.201600320
- [13] G. Gainza, J. Aguirre, J. Pedraz, R. Hernández, M. Igartua. *Eur. J. Pharm. Sci.*, **50** (3–4), 243 (2013). DOI: 10.1016/j.ejps.2013.07.003
- [14] T. Fujimura, A.D. Vilesov. RF Pat. № 2420350 *Mikrokapuly, soderzhashchie vodu ili vodnyj rastvor, (varianty) i sposoby ih polucheniya (varianty)*. Appl. 09.02.2009. Publ. 10.06.2011. (In Russian)
- [15] Section of the website of LLC „Diatech“: MIGRANT — is a new tool for treating wounds in the field in emergency situations. Text: electronic. URL: <http://www.diatehnn.ru> (In Russian)
- [16] Y.J. Lee, B. Javdan, A. Cowan, K. Front. *Cell Dev. Biol., Sec. Molecular and Cellular Pathology*, **11**, (2023). DOI: 10.3389/fcell.2023.1195600
- [17] R. Ghomi, S. Khalili, S. Khorasani, E. Neisiany, S. Ramakrishna. *Appl. Polym. Sci.*, **136**, 47738 (2019). DOI: 10.1002/app.4773
- [18] T.A. Kuznetsova, S.V. Polovov. *Marine Medicine*, **9** (4), 16 (2023). DOI: 10.22328/2413-5747-2023-9-4-16-25
- [19] T. Mosmann. *J. Immunol. Methods*, **65**(1–2), 55 (1983). DOI: 10.1016/0022-1759(83)90303-4
- [20] Roche Diagnostics GmbH. *Introduction of the RTCA SP Instrument. RTCA SP Instrument Operator's Manual* (ACEA Biosciences, Inc. 2008)
- [21] O.I. Aleksandrova, I.N. Okolov, Y.I. Khorolskaya, I.E. Panova, M.I. Blinova. *Ophthalmology in Russ.*, **15** (2), 167 (2018). DOI: 10.18008/1816-5095-2018-2-167-175
- [22] D.B. Trushina, R.A. Akasov, A.V. Khovankina, T.N. Borodina, T.V. Bukreeva, E.A. Markvicheva. *J. Mol. Liquids*, **284**, 215 (2019). DOI: 10.1016/j.molliq.2019.03.152
- [23] A.A. Abalymov, R.A. Verkhovskii, M.V. Novoselova, B.V. Parakhonskiy, D.A. Gorin, A.M. Yashchenok, G.B. Sukhorukov. *Biotechnol. J.*, **13** (11), 1800071 (2018). DOI: 10.1002/biot.201800071
- [24] N.N. Sudareva, O.M. Suvorova, V.D. Pautov. *Vestnik TvGU. Ser. Khimiya*, **35** (1), 147 (2019) (in Russian). DOI: 10.26456/vtchem2019.1.18
- [25] A.S. Timin, A.R. Muslimov, K.V. Lepik, O.S. Epifanovskaya, A.I. Shakirova, B.V. Afanasyev, B. Fehse, G.B. Sukhorukov. *Nanomedicine: Nanotechnology, Biology and Medicine*, **14** (1), 97 (2018). DOI: 10.1016/j.nano.2017.09.001
- [26] N.N. Sudareva, O.M. Suvorova, N.N. Saprykina, N.N. Shevchenko, K.A. Kolbe, V.K. Lavrentiev. *In: The Chemistry of Calcium Carbonate*. Ed. G.H.Hood. (Nova Sci. Publishers Inc., NY., 2022), p. 199.
- [27] G.I. Stein. *Rukovodstvo po konfokal'noj mikroskopii* (Izd-vo Politekh. un-ta Petra Velikogo, SPb., 2007) (in Russian)
- [28] A.D. Vilesov, O.V. Galibin, E.E. Zvartau, E.M. Krupitsky, E.F. Panarin, V.V. Thomson, I.V. Belozertseva, O.G. Genbach, O.A. Dravolina, L.P. Chukova. RF Pat. № 2462235. *Formulation of long-acting disulfiram and the method of its preparation*. Appl. 10.05.2011. Publ. 27.09.2012.
- [29] D.V. Volodkin, A.I. Petrov, M. Prevot, G.B. Sukhorukov. *Langmuir*, **20** (8), 3398 (2004). DOI: 10.1021/la036177z

Translated by A.Akhtyamov